Hawk-Pigeon Game Tactics for Unmanned Aerial Vehicle Swarm Target Defense

Wanying Ruan, Yongbin Sun, *Member, IEEE*, Yimin Deng, and Haibin Duan, *Senior Member, IEEE*

***Abstract*—Unmanned aerial vehicle (UAV) swarm target defense is a crucial and practical issue about group decision-making and cooperative control in multiagent systems. Hawk-pigeon game architecture is presented in this article to guide UAV swarm target defense. Firstly, a 6-degree-of-freedom UAV model is employed, and the control command converter is derived, which could be widely used in the transformation from the second-order integrator model to the 6-DOF UAV model. Moreover, the attack tactics and pursuit strategies of the defender UAVs are proposed inspired by the hawk's hunting mechanism, and the dynamic model of the attacker UAVs is formulated inspired by pigeon group homing behavior. Furthermore, the victory zone of the hawk-pigeon game is analyzed using the time of interception and explicitly exhibited in isochrones means. The proposed method is scalable and adaptive, adopting distributed decision-making to support large-scale UAV swarm engagement. Finally, comparative experiments in different scenarios demonstrate the effectiveness of the proposed method over state-of-the-art target-attacker-defender game methods on the win rate, the number of captures, and activity time.**

***Index Terms*—Hawk-pigeon game, swarm target defense, target-attacker-defender (TAD) game, unmanned aerial vehicle (UAV).**

I. Introduction

UNMANNED aerial vehicle (UAV) has been thriving in the civil, military, and other fields in recent years [1], [2]. UAV swarm target defense represents meaningful and challenging problems in industry and military practical applications, there is a typical UAV swarm target defense scenario where a swarm of invading UAVs attempts to destroy valuable assets, and a swarm of defending UAVs is required to intercept the intruders to defend assets. Situational awareness and assessment, dynamic task assignment [3], and cooperative decision-making and motion [4] are three key issues in the actual UAV swarm target defense process. In the context of accurate situational awareness and assessment, how to devise efficient tactics and strategies for a swarm of UAVs to prevail and accomplish specified tasks in the presence of an adversarial swarm of UAVs is an important project with practical application significance [5].

UAV swarm target defense problem belongs to the extending contents of the pursuit-evasion game [6], called the target-attacker-defender (TAD) game, which involves three players, namely target, attacker, and defender. The attacker aims to capture the target and the defender strives to intercept the attacker to protect the target from being captured by the attacker. The attacker can be divided into two types: suicidal and nonsuicidal attacker. The former only attacks the target, while the latter tries to evade the defender while attacking the target, which is considered in this article.

The differential game derived from the pursuit-evasion problem is widely used to analyze the TAD game. The active target defense differential games considering constrained or free players with identical or different abilities are analyzed in [7], [8], and [9], where the attacker is suicidal. A TAD game with a nonsuicidal attacker is considered in [10], where a cooperative strategy between the target and defender is provided, and the role switch for the attacker between the pursuit and evasion balances well [11]. Like these awesome works, most of the current research on the TAD game focuses on the case of one attacker, one target, and one defender. There are also some works on the multiplayer pursuit-evasion differential game, such as one evader and two pursuers [12], one evader and multiple pursuers [13], one pursuer and two evaders [14], one pursuer and multiple evaders [15], and multiple pursuers and multiple evaders [16], but the players move in the two-dimensional (2-D) Euclidean plane. With respect to the multiplayer reach-avoid differential game, the multiplayer reach-avoid differential game with obstacles in a 2-D domain using pairwise outcomes are provided by the graph-theoretic maximum matching algorithm and 4-D Hamilton–Jacobi–Isaacs (HJI) approach in [17]. Besides, a 3-D multiplayer reach-avoid game is decomposed into many multiple-pursuer and one-evader subgames using a maximum bipartite matching algorithm in [18], and the HJI equation value

Manuscript received 13 November 2022; revised 9 February 2023; accepted 15 February 2023. Date of publication 23 February 2023; date of current version 18 October 2023. This work was supported in part by the Science and Technology Innovation 2030-Key Project of "New Generation Artificial Intelligence" under Grant 2018AAA0100803, and in part by the National Natural Science Foundation of China under Grant U20B2071, Grant 91948204, Grant T2121003, Grant U1913602, and Grant 62103040. Paper no. TII-22-4672. *(Corresponding author: Haibin Duan.)*

Wanying Ruan, Yongbin Sun, and Yimin Deng are with the School of Automation Science and Electrical Engineering, Beihang University (BUAA), Beijing 100083, China (e-mail: wyruan@buaa.edu.cn; ybsuncookie@buaa.edu.cn; ymdeng@buaa.edu.cn).

Haibin Duan is with the School of Automation Science and Electrical Engineering, Beihang University (BUAA), Beijing 100083, China, and also with the Virtual Reality Fundamental Research Laboratory, Department of Mathematics and Theories, Peng Cheng Laboratory, Shenzhen 518000, China (e-mail: hbduan@buaa.edu.cn).

Color versions of one or more figures in this article are available at https://doi.org/10.1109/TII.2023.3248075.

Digital Object Identifier 10.1109/TII.2023.3248075

function of each subgame is computed in the game of degree. However, the player in these works is regarded as a first-order mass point. Generally, the differential game performs well when dealing with small-scale players but the solution is almost numerically intractable to solve when scaling it to the multiplayer game.

Reinforcement learning (RL) is an emerging artificial intelligence method. A frame of the TAD game using RL to train the attacker to actively avoid the defender while pursuing the target to obtain the optimal strategy is presented in [19]. The pursuit-evasion policy obtained by RL is developed in [20] for the UAV in one-to-one aerial combat, and the effectiveness of technologies in live flight experiments was examined [21]. However, it is difficult for RL to train to obtain a satisfactory solution because of the uncertainties. Besides, the Lyapunov-like method is proposed for the multiplayer game [22]. A multiplayer TAD game is formulated as multiple objectives in [23], where a modified Hungarian pairing algorithm and the control strategies adopting the Lyapunov-like method and the approximations of maximum and minimum functions are proposed, and a first-order particle model is used to simulate on the 2-D plane with promising results.

In this article, a novel multiplayer TAD game architecture is proposed from the perspective of bionics, which is highlighted by the swarm-to-swarm target defense using the UAV model in 3-D space. Biological behavior mechanisms [24] are meaningful not only because they provide better insights into animals' behavior [25], but also because intelligent autonomous platforms represented by UAVs will also perform tasks in a similar bionic mode [26]. Hawks and pigeons are predator-prey relationships [27], hawks use effective attack tactics and hunting strategies to capture prey [28], and pigeons can fly to their destination through coordinated movements [29] and effectively escape the threat of predators [30]. The intelligence and autonomy of the hawk and pigeon emerging in the dynamic game have enlightening significance to the UAV swarm confrontation, and the behavior mechanisms of the hawk and pigeon are worth further exploring. We attempt to model the relative mechanisms and apply them to UAV swarm target defense. The contributions and novelties of this article can be summarized as follows.

1) A 6-degree-of-freedom (6-DOF) UAV model is employed, which can simulate the motion of real fixed-wing aircraft relatively accurately and verify the practicability of the proposed approach. Moreover, a control command converter transforming the second-order integrator dynamics to the 6-DOF UAV model is derived.
2) A hawk-pigeon game architecture is proposed for UAV swarm target defense in 3-D space. The engagement tactics and control strategies of the defender UAVs are developed inspired by the hawk's targeting mechanism and pursuit strategy when hunting prey. The dynamic model of the attacker UAVs is formulated inspired by the pigeon's homing motion, which makes the attacker UAVs attack the target while avoiding the threat of the defender UAVs.
3) The victory zone of the hawk-pigeon game is analyzed. The estimated victory zones of the hawk and the pigeon, which are distinctly displayed using the isochrones, are obtained by calculating the time of interception. In the case of multiple hawks and pigeons, the initial conditions under which a certain number of pigeons are guaranteed to be captured are given.

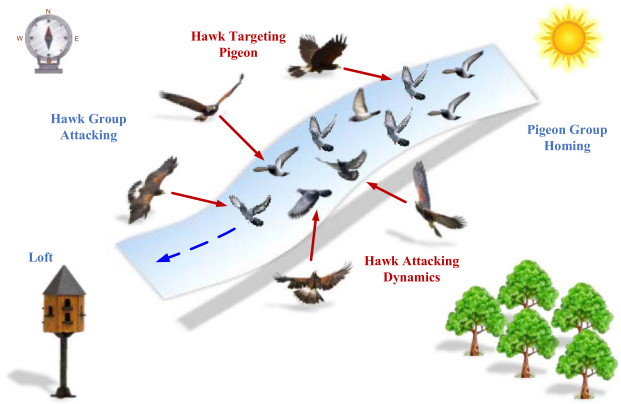

Fig. 1. Hawk-pigeon game schematic plot.

The rest of this article is organized as follows. Section II describes problem formulation. Section III introduces the hawk-pigeon game. Section IV analyzes the victory zone of the hawk-pigeon game. The comparative simulation results demonstrating the efficacy and superiority of our approach are shown in Section V. Finally, Section VI concludes this article.

II. Problem Formulation

A. Mapping Hawk-Pigeon Game to UAV Swarm Target Defense

The hawk-pigeon game schematic plot is illustrated in Fig. 1, depicting the scene where a flock of pigeons flies toward the loft while being attacked by hawks. UAV swarm target defense consists of the target, attackers, and defenders, where attackers aim to capture the target while escaping from defenders, and defenders aim to intercept attackers to protect the target. There are obvious similarities between the two, thus the hawk-pigeon game can be mapped to the UAV swarm target defense as follows: The loft is regarded as a static target asset, the hawks are assumed to be the defender UAVs (also called the hawk UAVs hereafter), and the pigeons are assumed to be the attacker UAVs (also called the pigeon UAVs hereafter). The strategies of attacker and defender UAVs can be designed drawing on the intelligence mechanism of pigeons and hawks.

Considering hawks and pigeons flying in 3-D space, the dynamic model of each hawk and pigeon is regarded as a second-order integrator model as

$$\begin{cases} \dot{\mathbf{p}} = \mathbf{v} \\ \dot{\mathbf{v}} = \mathbf{u} \end{cases} \tag{1}$$

where $\mathbf{p} \in \mathbb{R}^3$ is the position vector and $\mathbf{v} \in \mathbb{R}^3$ is the velocity vector. $\mathbf{u} \in \mathbb{R}^3$ is the acceleration control command, which can be represented as $\mathbf{u} = [u_x, u_y, u_z]^{\mathrm{T}}$.

Remark 1: Soft capture is considered in this article, that is, the capture happens when the distance between two sides is

less than the capture range D_C. It is stipulated that the victory belongs to the pigeon UAVs as long as one pigeon UAV captures the target, however, hawk UAVs have to capture all pigeon UAVs before the pigeon UAVs capture the target to win.

B. UAV Model

The UAV model adopted in this article is a 6-DOF aircraft model simulating fixed-wing aircraft motion. The aircraft's state and attitude, including roll, pitch, yaw, and complex aerial maneuvers during engagements, are computed in a way that realistically simulates the aircraft's performance capabilities without the need for full aerodynamics modelling. The hawk UAVs and pigeon UAVs are modelled as the same 6-DOF aircraft model to verify the effectiveness and practicability of the proposed approach.

Considering the earth-surface inertial reference frame, the z-axis is positive upwards. The dynamic and kinematic equations of the 6-DOF UAV model [31] are described as

$$\begin{cases} \dot{x} = V\cos\mu\cos\varphi \\ \dot{y} = V\cos\mu\sin\varphi \\ \dot{z} = V\sin\mu \\ \dot{V} = g\left(n_x - \sin\mu\right) \\ \dot{\mu} = g\left(n_f\cos\gamma - \cos\mu\right)/V \\ \dot{\varphi} = gn_f\sin\gamma/\left(V\cos\mu\right) \end{cases} \tag{2}$$

where $\mathbf{p} = [x, y, z]^T$ denotes the position vector and $\mathbf{v} = [\dot{x}, \dot{y}, \dot{z}]^T$ denotes the velocity vector. $[V, \mu, \varphi]$ are the airspeed, flight path angle, and heading angle, respectively. $[n_x, n_f, \gamma]$ are longitudinal load factor, normal load factor, and bank angle, respectively, which are the control inputs of the 6-DOF UAV model. $g = 9.8\ \mathrm{m/s^2}$ is the acceleration of gravity.

It is assumed that the UAVs are equipped with omnidirectional sensors, and the sensing region is modelled as a sphere with a sensing radius R_s. The UAVs can obtain the state information of the UAVs within the sensing radius.

C. Control Command Converter

To apply the control laws designed based on the second-order integrator model in (1) to the 6-DOF UAV model, it is necessary to design a control command converter to convert the acceleration control command of the second-order integrator model into the longitudinal load factor, normal load factor, and bank angle control command of the 6-DOF UAV model.

Taking the second derivative of the 3-D positions of the 6-DOF UAV model given by (2), it can be obtained that

$$\begin{aligned} \begin{bmatrix} \ddot{x} \\ \ddot{y} \\ \ddot{z} \end{bmatrix} &= \begin{bmatrix} \cos\mu\cos\varphi & -\sin\mu\cos\varphi & -\cos\mu\sin\varphi \\ \cos\mu\sin\varphi & -\sin\mu\sin\varphi & \cos\mu\cos\varphi \\ \sin\mu & \cos\mu & 0 \end{bmatrix} \\ &\quad \times \begin{bmatrix} \dot{V} \\ V\dot{\mu} \\ V\dot{\varphi} \end{bmatrix} \\ &\triangleq \begin{bmatrix} u_x \\ u_y \\ u_z \end{bmatrix} = M \begin{bmatrix} g\left(n_x - \sin\mu\right) \\ g\left(n_f\cos\gamma - \cos\mu\right) \\ gn_f\sin\gamma/\cos\mu \end{bmatrix} \end{aligned}$$

$$\Rightarrow M^{-1}\begin{bmatrix} u_x/g \\ u_y/g \\ u_z\cos\mu/g \end{bmatrix} + \begin{bmatrix} \sin\mu \\ \cos\mu \\ 0 \end{bmatrix} = \begin{bmatrix} n_x \\ n_f\cos\gamma \\ n_f\sin\gamma \end{bmatrix} \triangleq \Gamma \tag{3}$$

where M represents the transformation matrix and Γ represents an equivalent vector. Therefore, the control command converter can be derived as follows:

$$n_x = \Gamma(1) \tag{4}$$

$$\gamma = \tan^{-1}\left(\Gamma(3)/\Gamma(2)\right) \tag{5}$$

$$n_f = \begin{cases} \Gamma(2)/\cos\gamma & \text{if } \sin\gamma = 0 \\ \Gamma(3)/\sin\gamma & \text{if} \cos\gamma = 0 \end{cases}. \tag{6}$$

The control input commands $[n_x, n_f, \gamma]$ of the 6-DOF UAV model have been solved. Hence, we can obtain $[n_x, n_f, \gamma]$ to control the 6-DOF UAV model according to the control inputs $[u_x, u_y, u_z]$ of the second-order integrator model.

III. Hawk-Pigeon Game

In this section, the hawk's attack targeting selection mechanisms are modelled and used as the attack tactics of the hawk UAV swarm. The hawk's attack dynamics are modelled and served as the pursuit strategy of the hawk UAV swarm. The pigeon's homing motion mechanisms are modelled and employed to design the control strategy of the pigeon UAV swarm.

A. Modelling Hawk's Attack Tactics: Targeting Mechanism

Biological studies indicate that the defensive advantages of prey groups can be reduced when predators adopt sophisticated attack tactics and targeting mechanisms. Through observation experiments on the hawk's hunting behavior, the hawk's targeting mechanisms can be modelled as three criteria: proximity criterion; margin criterion; and density criterion [32].

Proximity criterion: The hawk chooses the closest pigeon as its attack target. The targeting mechanism based on the proximity criterion is modelled as

$$\begin{cases} T^1_{\text{pigeon}} = \arg\min\limits_{j\in Z_1}\left(\left\|\mathbf{p}_{\text{hawk}} - \mathbf{p}^j_{\text{pigeon}}\right\|\right) \\ Z_1 = \left\{j \,\middle|\, \left\|\mathbf{p}_{\text{hawk}} - \mathbf{p}^j_{\text{pigeon}}\right\| \le R_s\right\} \end{cases} \tag{7}$$

where T^1_{pigeon} is the nearest target pigeon selected by the hawk, $\mathbf{p}_{\text{hawk}}$ is the position vector of the hawk, $\mathbf{p}^j_{\text{pigeon}}$ is the position vector of the jth pigeon, and R_s is the sensing radius.

Margin Criterion: The hawk selects the most peripheral pigeon as its attack target. The peripherality of the jth pigeon is defined as the average of the position vectors from the hawk toward all the jth pigeon's neighbors. The marginal angle of the jth pigeon is defined as the angle between its peripherality vector and the vector pointing from the hawk's position to the jth pigeon's position. The pigeon that is the most marginal is the individual with the maximum marginal angle. The targeting

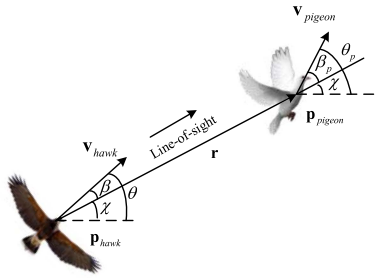

Fig. 2. Hawk-pigeon game geometry.

mechanism based on the margin criterion is modelled as

$$\begin{cases} T^2_{\text{pigeon}} = \arg\max\limits_{j\in Z_1} \left(\left\langle \frac{\mathbf{p}^j_{\text{pigeon}} - \mathbf{p}_{hawk}}{\left\|\mathbf{p}^j_{\text{pigeon}} - \mathbf{p}_{\text{hawk}}\right\|}, \frac{\mathbf{q}^j_{\text{pigeon}}}{\left\|\mathbf{q}^j_{\text{pigeon}}\right\|} \right\rangle \right) \\ Z_1 = \left\{ j \,\middle|\, \left\|\mathbf{p}_{\text{hawk}} - \mathbf{p}^j_{\text{pigeon}}\right\| \le R_s \right\} \\ \mathbf{q}^j_{\text{pigeon}} = \frac{1}{N_m} \sum_{m\in Z_2} \left(\mathbf{p}^m_{\text{pigeon}} - \mathbf{p}_{\text{hawk}}\right) / \left\|\mathbf{p}^m_{\text{pigeon}} - \mathbf{p}_{\text{hawk}}\right\| \\ Z_2 = \left\{ m \,\middle|\, \left\|\mathbf{p}^j_{\text{pigeon}} - \mathbf{p}^m_{\text{pigeon}}\right\| \le R_{\text{nei}}, m \ne j \right\} \end{cases} \tag{8}$$

where T^2_{pigeon} is the most margined target pigeon selected by the hawk, $\langle\cdot\rangle$ is used to calculate the angle between two vectors, $\mathbf{q}^j_{\text{pigeon}}$ represents the peripherality vector for the jth pigeon, R_{nei} is the pigeon's neighborhood radius, and N_m is the number of pigeons within the neighborhood radius of the observed pigeon.

Density Criterion: The hawk targets the pigeon located in the densest area. The pigeon with more neighbors and closer to the center of neighbors can be considered as the individual in the densest area. This kind of individual is surrounded by many neighbors, which can facilitate successive attacks for the hawk. The targeting mechanism based on the density criterion is modelled as

$$\begin{cases} T^3_{\text{pigeon}} = \arg\max\limits_{j\in Z_1} \left(\left\|\mathbf{p}^j_{\text{pigeon}} - \mathbf{p}^{j\_c}_{\text{pigeon}}\right\| \Big/ \left(1 + \exp\left(-N_d\right)\right) \right) \\ Z_1 = \left\{ j \,\middle|\, \left\|\mathbf{p}_{\text{hawk}} - \mathbf{p}^j_{\text{pigeon}}\right\| \le R_s \right\} \\ \mathbf{p}^{j\_c}_{\text{pigeon}} = \sum_{m\in Z_3} \mathbf{p}^m_{\text{pigeon}} / N_d \\ Z_3 = \left\{ m \,\middle|\, \left\|\mathbf{p}^j_{\text{pigeon}} - \mathbf{p}^m_{\text{pigeon}}\right\| \le R_{\text{nei}}, m \ne j \right\} \end{cases} \tag{9}$$

where T^3_{pigeon} is the target pigeon selected by the hawk according to the density criteria, $\mathbf{p}^{j\_c}_{\text{pigeon}}$ represents the position center of all neighbors of the jth pigeon, and N_d is the number of pigeons within the neighborhood radius of the observed pigeon.

Based on three targets selected by the hawk's targeting mechanism, the situation assessment function is designed to determine the final attack target. Fig. 2 shows the relative situation geometry between hawk and pigeon. The situation assessment function incorporates contributions of orientation and range [33].

The contribution of orientation S_o is shown as follows. The hawk aims to minimize β and β_p. The larger the S_o, the more favorable for the hawk to attack the pigeon

$$S_O = 1 - (\beta + \beta_p)/\pi. \tag{10}$$

The contribution of the range S_R is shown as follows. The hawk's objective is maximizing S_R

$$S_R = \exp\left(-(r - D_C)^2 \Big/ 2D_C^2\right) \tag{11}$$

where D_C is the capture range.

Combining both these two contributions, the final situation assessment function S_{OR} is yielded by multiplying S_O and S_R shown as follows:

$$S_{OR} = S_O S_R. \tag{12}$$

The S_{OR} of the hawk's targeted three target pigeons (T^1_{pigeon}, T^2_{pigeon}, T^3_{pigeon}) are calculated, and the pigeon with the maximum S_{OR} is selected as the final attack target.

Remark 2: The hawk UAV swarm applies a "divide-and-conquer one by one" attack tactic toward the pigeon UAV swarm, which means that one hawk UAV targets only one pigeon UAV per attack, and the target remains unchanged for the duration of the attack until the current target pigeon UAV is successfully captured, then the hawk UAV attacks the next target pigeon UAV.

B. Modelling Harris' Hawk Pursuit Strategy

Once a target prey is determined, hawks will adopt swift and violent pursuit strategies to hunt the prey. Brighton and Taylor, from the University of Oxford's Department of Zoology, have been researching the attack strategies in birds of prey [34]. They conducted flight tests on five Harris' Hawks, and the data results show that the linear combined guidance law of proportional navigation (PN) and proportional pursuit (PP) can best model Harris' Hawks' attack dynamics chasing maneuvering lure. Inspired by the attack dynamics mechanism of Harris' Hawk, the pursuit control strategy of hawk UAVs can be designed.

The attack dynamics of Harris' Hawk can be analyzed according to the pursuit geometry of the hawk chasing a pigeon as shown in Fig. 2, where $\mathbf{p}_{\text{hawk}}$ and $\mathbf{p}_{\text{pigeon}}$ are the position vectors of the hawk and pigeon, respectively. $\mathbf{v}_{\text{hawk}}$ and $\mathbf{v}_{\text{pigeon}}$ are velocity vectors of the hawk and pigeon, respectively. $\mathbf{r}$ is the line-of-sight (LOS) vector from the hawk to the pigeon, $\|\mathbf{r}\| = r$. θ and θ_p are the heading angles of the hawk and pigeon with respect to the reference frame, respectively. β is the deviation angle between the hawk's velocity vector and the LOS vector. β_p is the deviation angle between the pigeon's velocity vector and the LOS vector. χ is the LOS angle.

The turning rate is taken as the control variable. Concerning the PN, the turning rate is proportional to the LOS angle rate. Concerning the PP, the turning rate is proportional to the deviation angle between the hawk's velocity vector and the LOS vector. The Harris' Hawk's attack dynamics can be modelled as follows [34]:

$$\dot{\theta} = K_{\text{PN}}\dot{\chi} - K_{\text{PP}}\beta \tag{13}$$

where $\dot{\theta}$ is the hawk's turning rate, $\dot{\chi}$ is the LOS angle rate, $K_{\text{PN}} \ge 0$ is the feedback gain of PN, and $K_{\text{PP}} \ge 0$ is the feedback gain of PP. The purpose of PP is to make the deviation angle β approach zero. PN at $K_{\text{PN}} = 1$ indicates that the turning rate $\dot{\theta}$ is equal to the LOS angle rate $\dot{\chi}$, which means that the deviation angle β maintains unchanged, under this condition,

when the initial deviation angle $\beta = 0$, PN is equivalent to the pure pursuit, when the initial deviation angle $\beta \neq 0$, PN is equivalent to deviated pure pursuit.

Transferring the scalar turning rate to the acceleration vector, Harris' Hawk's attack dynamics can be generalized to the 3-D case [34], which can be rewritten in vector form as

$$\mathbf{u}_{\text{hawk}} = K_{\text{PN}}\boldsymbol{\omega} \times \mathbf{v}_{\text{hawk}} - K_{\text{PP}}\boldsymbol{\beta} \times \mathbf{v}_{\text{hawk}} \tag{14}$$

$$\boldsymbol{\omega} = (\mathbf{p}_{\text{pigeon}} - \mathbf{p}_{\text{hawk}}) \times (\mathbf{v}_{\text{pigeon}} - \mathbf{v}_{\text{hawk}}) \Big/ \|\mathbf{p}_{\text{pigeon}} - \mathbf{p}_{\text{hawk}}\|^2 \tag{15}$$

$$\boldsymbol{\beta} = \cos^{-1}\left(\frac{(\mathbf{p}_{\text{pigeon}} - \mathbf{p}_{\text{hawk}}) \cdot \mathbf{v}_{\text{hawk}}}{\|\mathbf{p}_{\text{pigeon}} - \mathbf{p}_{\text{hawk}}\| \, \|\mathbf{v}_{\text{hawk}}\|}\right) \times \left(\frac{(\mathbf{p}_{\text{pigeon}} - \mathbf{p}_{\text{hawk}}) \times \mathbf{v}_{\text{hawk}}}{\|(\mathbf{p}_{\text{pigeon}} - \mathbf{p}_{\text{hawk}}) \times \mathbf{v}_{\text{hawk}}\|}\right) \tag{16}$$

where $\mathbf{u}_{\text{hawk}}$ is the hawk's control acceleration vector, $\|\mathbf{u}_{\text{hawk}}\| = \|\dot{\theta}\|\|\mathbf{v}_{\text{hawk}}\|$. $\boldsymbol{\omega}$ is the angular velocity of LOS vector $\mathbf{r}$, $\|\boldsymbol{\omega}\| = \|\dot{\chi}\|$. $\boldsymbol{\beta}$ is the deviation angle vector form of β normal to $\mathbf{r}$ and $\mathbf{v}_{\text{hawk}}$, $\|\boldsymbol{\beta}\| = \|\beta\|$.

During the hunt, hawks adjust their pursuit strategies according to the different escape styles of prey. Therefore, an adaptive gain adjustment mechanism for hawk's attack dynamics is designed as follows:

$$\begin{cases} K_{\text{PN}} = \exp\left(-\|\boldsymbol{\beta}\|\right) \\ K_{\text{PP}} = g\,\|\boldsymbol{\beta}\| \end{cases} \tag{17}$$

where $g = 9.8\ \text{m/s}^2$ is the acceleration of gravity.

The modelling of the adaptive pursuit strategies inspired by Harris' Hawk's attack dynamic mechanism for defender UAV swarm has been completed and summarized in (14)–(17).

Remark 3: Generally, the feedback gains K_{PN} and K_{PP} are constants specified manually according to experience or substantial tests, which can work for specific scenarios but are not well-suitable for the dynamic task. The adaptive gain adjustment mechanism in (17) is designed based on a simple idea. The deviation angle β is an important variable for pursuit. When β is large, PP plays a dominant role and quickly adjusts the heading to point to the prey. When β is small, PN and PP coordinate and accurately adjust the heading to closely chasing the prey. Hence, the gains can adaptively adjust to the real-time situation of the hawk and prey for fast and accurate capture.

C. Pigeon Group Homing Dynamics Model

Three control components are designed to simulate the pigeon group homing dynamics: the motion toward the loft, the motion to escape from predators, and the motion to prevent collisions between pigeons. Therefore, the control strategy for each pigeon can be designed as follows [35]:

$$\mathbf{u}_{\text{pigeon}} = \mathbf{u}_{\text{pigeon}}^{\text{attack}} + \mathbf{u}_{\text{pigeon}}^{\text{escape}} + \mathbf{u}_{\text{pigeon}}^{\text{avoid}} \tag{18}$$

where $\mathbf{u}_{\text{pigeon}}$ is the pigeon's total acceleration control command, $\mathbf{u}_{\text{pigeon}}^{\text{attack}}$ represents loft attraction control component, $\mathbf{u}_{\text{pigeon}}^{\text{escape}}$ represents the control component of escaping from predators, and $\mathbf{u}_{\text{pigeon}}^{\text{avoid}}$ represents the control component of avoiding the collision.

The loft attraction control component $\mathbf{u}_{\text{pigeon}}^{\text{attack}}$ is shown as follows, which leads each pigeon to the target asset *T*, i.e., the loft. Pigeons are accelerated by the attraction of the target and engage in a greedy attack strategy against the target, producing a motion similar to pure pursuit. It corresponds to the attack control strategy of pigeon UAVs toward the target asset in the UAV swarm target defense.

$$\mathbf{u}_{\text{pigeon}}^{\text{attack}} = k_1(\mathbf{p}_T - \mathbf{p}_{\text{pigeon}})/\|\mathbf{p}_T - \mathbf{p}_{\text{pigeon}}\| \tag{19}$$

where $\mathbf{p}_{\text{pigeon}}$ is the position vector of the observed pigeon, $\mathbf{p}_T$ is the position vector of the target, and $k_1 > 0$ is the attraction acceleration gain of the target.

The control component of escaping from predators $\mathbf{u}_{\text{pigeon}}^{\text{escape}}$ is shown as follows, which simulates the pigeon's tendency to escape from the predator. The component only occurs when predators pose threats to the pigeon, that is when there is any predator within the pigeon's escaping safety radius. It corresponds to the control strategy of the pigeon UAV escaping from the hawk UAV in the UAV swarm target defense

$$\begin{cases} \mathbf{u}_{\text{pigeon}}^{\text{escape}} = \sum_{j\in E_2} k_2^j \left(\mathbf{p}_{\text{pigeon}} - \mathbf{p}_{\text{hawk}}^j\right) \Big/ \left\|\mathbf{p}_{\text{pigeon}} - \mathbf{p}_{\text{hawk}}^j\right\| \\ k_2^j = \exp\left(1 + \left(\left\|\mathbf{p}_{\text{pigeon}} - \mathbf{p}_{\text{hawk}}^j\right\| - R_E\right)^2 \Big/ R_E^2\right) \\ E_2 = \left\{ j \,\middle|\, \left\|\mathbf{p}_{\text{pigeon}} - \mathbf{p}_{\text{hawk}}^j\right\| \le R_E \right\} \end{cases} \tag{20}$$

where $\mathbf{p}_{\text{hawk}}^j$ is the position vector of the *j*th hawk and R_E is the pigeon's escaping safety radius.

The control component of avoiding collision $\mathbf{u}_{\text{pigeon}}^{\text{avoid}}$ is shown as follows, which helps pigeons avoid collisions with other pigeons. This component only works if there are other pigeons within the avoiding collision safety radius for the observed pigeon. It corresponds to the control strategy of the pigeon UAV to avoid collision with other pigeon UAVs in the UAV swarm target defense

$$\begin{cases} \mathbf{u}_{\text{pigeon}}^{\text{avoid}} = \sum_{j\in E_3} k_3^j \left(\mathbf{p}_{\text{pigeon}} - \mathbf{p}_{\text{pigeon}}^j\right) \Big/ \left\|\mathbf{p}_{\text{pigeon}} - \mathbf{p}_{\text{pigeon}}^j\right\| \\ k_3^j = \left(R_A - \left\|\mathbf{p}_{\text{pigeon}} - \mathbf{p}_{\text{pigeon}}^j\right\|\right) \Big/ R_A \\ E_3 = \left\{ j \,\middle|\, \left\|\mathbf{p}_{\text{pigeon}} - \mathbf{p}_{\text{pigeon}}^j\right\| \le R_A \right\} \end{cases} \tag{21}$$

where $\mathbf{p}_{\text{pigeon}}^j$ is the position vector of the *j*th pigeon and R_A is the pigeon's avoiding collision safety radius.

The dynamics model of the attacker UAV swarm inspired by pigeon group homing behavior has been formulated.

IV. Hawk-Pigeon Game Analysis: Estimation of Victory Zone

The victory zone (*VZ*) refers to the initial positions where victory can be guaranteed. The mathematical definitions can be presented as follows:

$$VZ_{\text{hawk}}^{\mathbf{p}_{\text{pigeon}}^0} = \left\{ \mathbf{p}_{\text{hawk}}^0 \,\middle|\, \left\|\mathbf{p}_{\text{hawk}}^f - \mathbf{p}_{\text{pigeon}}^f\right\| \le D_C \,\&\, \left\|\mathbf{p}_{\text{pigeon}}^f - \mathbf{p}_T\right\| > D_C \right\} \tag{22}$$

$$VZ_{\text{pigeon}}^{\mathbf{p}_{\text{hawk}}^0} = \left\{ \mathbf{p}_{\text{pigeon}}^0 \left| \left\| \mathbf{p}_{\text{pigeon}}^f - \mathbf{p}_T \right\| \right. \right. \\ \left. \left. \leq D_C \& \left\| \mathbf{p}_{\text{hawk}}^f - \mathbf{p}_{\text{pigeon}}^f \right\| > D_C \right\} \tag{23}$$

where $VZ_{\text{hawk}}^{\mathbf{p}_{\text{pigeon}}^0}$ is the victory zone of the hawk for a given pigeon's initial position $\mathbf{p}_{\text{pigeon}}^0$ and $VZ_{\text{pigeon}}^{\mathbf{p}_{\text{hawk}}^0}$ is the victory zone of the pigeon for a given hawk's initial position $\mathbf{p}_{\text{hawk}}^0$. $\mathbf{p}_{\text{hawk}}^f$ and $\mathbf{p}_{\text{pigeon}}^f$ are the final positions of the hawk and pigeon, respectively, at the end of the game.

The victory zone for the hawk and the pigeon can be estimated in terms of the time of interception under assumption 1 [23], [36]. Theorem 1 gives the time of interception for the hawk to capture a pigeon, which is the basis to estimate the victory zone. The estimated victory zone can guide the winning conditions for both sides.

Assumption 1: Suppose $V_{\text{pigeon}}^{\max} < V_{\text{hawk}}^{\max}$, the pigeon attacks the target with maximum speed $V_{\text{pigeon}}^{\max}$ only attracted by the target without other drives, and the initial velocity points toward the target. The hawk pursues the pigeon with maximum speed $V_{\text{hawk}}^{\max}$, and its initial velocity points toward the pigeon.

Theorem 1: Based on Assumption 1, given the initial positions of the hawk and the pigeon, the hawk adopts Harris' Hawk's pursuit strategy described in (14)–(17), and the time of interception for the hawk to capture the pigeon is given by

$$t_{\text{HP}} = \frac{r_{\text{HP}}^0 \left(\cos\left(\beta_p^0 + \beta\right) + C_V \right) - D_C \left(\cos\left(\beta_p^f + \beta\right) + C_V \right)}{V_{\text{pigeon}}^{\max} \cos\beta \left(C_V^2 - 1 \right)} \tag{24}$$

where t_{HP} is the time of interception for the hawk to capture the pigeon, $r_{\text{HP}}^0 = \|\mathbf{p}_{\text{hawk}}^0 - \mathbf{p}_{\text{pigeon}}^0\|$ is the initial distance between the hawk and the pigeon, β_p^0 is the initial deviation angle between the pigeon's velocity vector and the LOS vector, and β_p^f is the final deviation angle between the pigeon's velocity vector and the LOS vector when the pigeon is captured by the hawk, $\cos\beta \neq 0$, $C_V = V_{\text{hawk}}^{\max}/V_{\text{pigeon}}^{\max}$.

Proof: As shown in Fig. 2, the dynamics equations can be given by

$$\begin{cases} \dot{r} = V_{\text{pigeon}}^{\max} \cos\beta_p - V_{\text{hawk}}^{\max} \cos\beta \\ r\dot{\chi} = V_{\text{pigeon}}^{\max} \sin\beta_p - V_{\text{hawk}}^{\max} \sin\beta \end{cases}. \tag{25}$$

Since θ_p remains unchanged, $\dot{\theta}_p = 0$, and $\theta_p = \chi + \beta_p$, so $\dot{\beta}_p = -\dot{\chi}$. Rewriting (25) as follows:

$$\dot{r} = V_{\text{pigeon}}^{\max} \cos\beta_p - V_{\text{hawk}}^{\max} \cos\beta \tag{26}$$

$$\dot{\beta}_p = -\dot{\chi} = \left(-V_{\text{pigeon}}^{\max} \sin\beta_p + V_{\text{hawk}}^{\max} \sin\beta \right)/r. \tag{27}$$

Further, (27) can be equivalently written as follows:

$$r\dot{\beta}_p = -V_{\text{pigeon}}^{\max} \sin\beta_p + V_{\text{hawk}}^{\max} \sin\beta. \tag{28}$$

Multiplying (26) by $\cos(\beta_p + \beta)$, we have

$$\dot{r} \cos\left(\beta_p + \beta\right) = V_{\text{pigeon}}^{\max} \cos\beta_p \cos\left(\beta_p + \beta\right) \\ - V_{\text{hawk}}^{\max} \cos\beta \cos\left(\beta_p + \beta\right). \tag{29}$$

Multiplying (28) by $\sin(\beta_p + \beta)$, we have

$$r\dot{\beta}_p \sin\left(\beta_p + \beta\right) = -V_{\text{pigeon}}^{\max} \sin\beta_p \sin\left(\beta_p + \beta\right) \\ + V_{\text{hawk}}^{\max} \sin\beta \sin\left(\beta_p + \beta\right). \tag{30}$$

Subtracting (30) from (29), it can be obtained that

$$\begin{aligned} &\dot{r} \cos\left(\beta_p + \beta\right) - r\dot{\beta}_p \sin\left(\beta_p + \beta\right) \\ &= V_{\text{pigeon}}^{\max} \cos\beta_p \cos\left(\beta_p + \beta\right) + V_{\text{pigeon}}^{\max} \sin\beta_p \sin\left(\beta_p + \beta\right) \\ &\quad - \left(V_{\text{hawk}}^{\max} \cos\beta \cos\left(\beta_p + \beta\right) + V_{\text{hawk}}^{\max} \sin\beta \sin\left(\beta_p + \beta\right) \right) \\ &= V_{\text{pigeon}}^{\max} \cos\beta - V_{\text{hawk}}^{\max} \cos\beta_p \\ &\Rightarrow \dot{r} \cos\left(\beta_p + \beta\right) - r\dot{\beta}_p \sin\left(\beta_p + \beta\right) \\ &\quad + V_{\text{hawk}}^{\max} \cos\beta_p = V_{\text{pigeon}}^{\max} \cos\beta. \end{aligned} \tag{31}$$

According to (26), substituting $C_V(\dot{r} + V_{\text{hawk}}^{\max} \cos\beta)$ for $V_{\text{hawk}}^{\max} \cos\beta_p$in (31), it can be obtained that

$$\begin{aligned} &\dot{r} \cos\left(\beta_p + \beta\right) - r\dot{\beta}_p \sin\left(\beta_p + \beta\right) + \dot{r}C_V + C_V V_{\text{hawk}}^{\max} \cos\beta \\ &\quad = V_{\text{pigeon}}^{\max} \cos\beta \\ &\Rightarrow \frac{d}{dt}\left(r\left(\cos\left(\beta_p + \beta\right) + C_V \right) \right) = V_{\text{pigeon}}^{\max} \cos\beta \\ &\quad - C_V V_{\text{hawk}}^{\max} \cos\beta \\ &\Rightarrow \frac{d}{dt}\left(r\left(\cos\left(\beta_p + \beta\right) + C_V \right) \right) = V_{\text{pigeon}}^{\max} \cos\beta \left(1 - C_V^2 \right). \end{aligned} \tag{32}$$

Integrating (32), the time of interception for the hawk to capture the pigeon represented as in (24) can be obtained. ■

Remark 4: The time of interception represented as in (24) is also suitable to the situation where the hawk adopts the deviated pure pursuit. More generally, in the pursuit-evasion game with a nonmaneuvering evader, when β is constant (including $\beta = 0$), the time of interception given by Theorem 1 still holds.

For the given initial positions of the pigeon and the target, the time of interception for the pigeon capturing the target can be given by

$$t_{PT} = \left(r_{PT}^0 - D_C \right) / V_{\text{pigeon}}^{\max} \tag{33}$$

where t_{PT} is the time of interception for the pigeon capturing the target. $r_{PT}^0 = \|\mathbf{p}_{\text{pigeon}}^0 - \mathbf{p}_T\|$ is the initial distance between the pigeon and the target.

The estimated victory zone can be obtained according to the time difference between the interception time of the hawk capturing the pigeon and the pigeon capturing the target, the time difference is as follows:

$$t_F = t_{PT} - t_{\text{HP}}. \tag{34}$$

The hawk would win the game if $t_{PT} > t_{\text{HP}}$, conversely, the pigeon would win the game if $t_{PT} < t_{\text{HP}}$. From the perspective of the isochrones of t_F, the zone with $t_F > 0$ is the estimated hawk's victory zone, and the zone with $t_F < 0$ is the estimated pigeon's victory zone.

For the sake of brevity, we analyze the situation on the 2-D plane and draw the isochrones to explicitly show the estimated victory zone of the hawk and the pigeon. The isochrones

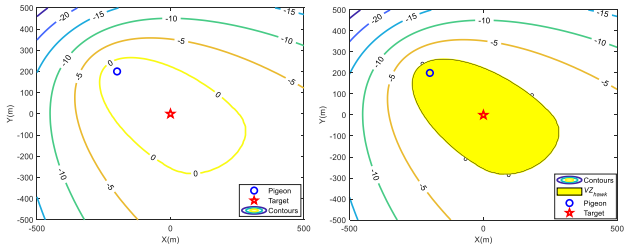

(a) (b)

Fig. 3. Isochrones of t_F and the estimated victory zone of the hawk given the pigeon's initial position. (a) Isochrones of t_F. (b) Estimated victory zone of the hawk (VZ_{hawk}).

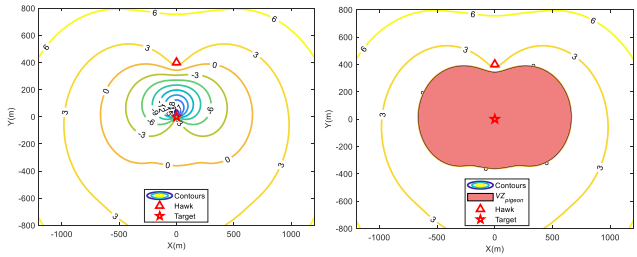

(a) (b)

Fig. 4. Isochrones of t_F and the estimated victory zone of the pigeon given the hawk's initial position. (a) Isochrones of t_F. (b) Estimated victory zone of the pigeon (VZ_{pigeon}).

can be obtained by evaluating t_F for different initial positions of the hawk and the pigeon. The parameters are set as follows: $V_{\text{pigeon}}^{\max} = 350$ km/h; $V_{\text{hawk}}^{\max} = 400$ km/h; $D_C = 10$ m, $dt = 0.01$ s; and $\mathbf{p}_T = [0, 0]$m. For the pigeon's initial position $\mathbf{p}_{\text{pigeon}}^0 = [-200, 200]$m, and the isochrones of t_F are drawn in Fig. 3, in which the zone with isochrones of $t_F > 0$ denotes the hawk's estimated victory zone, i.e., the yellow zone VZ_{hawk} in Fig. 3(b). For the hawk's initial position $\mathbf{p}_{\text{hawk}}^0 = [0, 400]$m, the isochrones of t_F are drawn in Fig. 4, in which the zone with isochrones of $t_F < 0$ denotes the pigeon's estimated victory zone, i.e., the pink zone VZ_{pigeon} in Fig. 4(b).

The estimated victory zone is obtained under certain conditions but is not the real victory zone. Since the strategies and the motions of the hawk and the pigeon are time-varying and uncertain, the exact real victory zone cannot be solved as the game progresses dynamically. While some victory conditions can be inferred from the estimated victory zone. It is the best situation for the pigeon to capture the target in a straight line at maximum speed. Whereas, in practice, the pigeon may escape the threat of the hawk by employing the control strategy described in (18)–(21), so the pigeon needs more time to capture the target or even fails to capture the target, which gives the hawk more opportunities and wider space to hunt, resulting in expanding its victory zone. Therefore, the conclusion about the victory zone can be inferred as follows: The real victory zone of the hawk is at least the estimated victory zone, conversely, the real victory zone of the pigeon is, at best, the estimated victory zone.

The conclusion about the victory zone can be demonstrated by Monte Carlo simulations. The pigeon employs the control strategy described in (18)–(21), the relevant parameters are given

TABLE I
SIMULATION PARAMETERS

Parameters	Description	Value
D_C (m)	Capture range	10
R_s (km)	Sensing radius	1
R_{nei} (m)	Pigeon's neighborhood radius	100
k_1	Attraction acceleration gain of the target	1
R_E (m)	Pigeon's escaping radius	100
R_A (m)	Pigeon's avoiding collision radius	20
$V_{\text{pigeon}}^{\min}$, $V_{\text{pigeon}}^{\max}$ (km/h)	Limited speed scope of pigeon UAV	50,350
$V_{\text{hawk}}^{\min}$, $V_{\text{hawk}}^{\max}$ (km/h)	Limited speed scope of hawk UAV	50,400

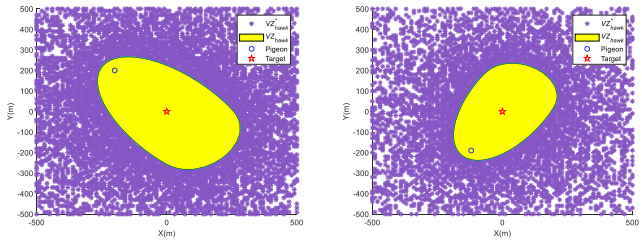

Fig. 5. Real victory zone and the estimated victory zone for the hawk under different conditions.

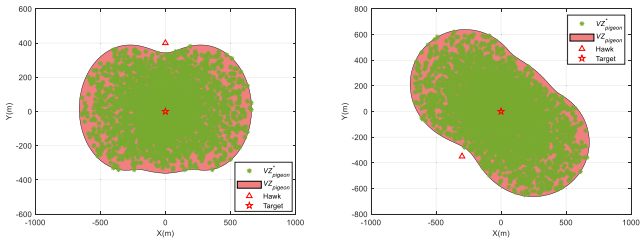

Fig. 6. Real victory zone and the estimated victory zone for the pigeon under different conditions.

in Table I. The initial positions of the hawk and the pigeon are set randomly. Some simulation results are given in Figs. 5 and 6. In Fig. 5, the purple asterisk markers denote the hawk's real victory zone VZ_{hawk}^*, and the yellow zone is the estimated victory zone VZ_{hawk}. The simulation results demonstrate that the hawk's real victory zone covers completely and exceeds the estimated victory zone, i.e., $VZ_{\text{hawk}}^* \geq VZ_{\text{hawk}}$. In Fig. 6, the dark green asterisk markers denote the pigeon's real victory zone VZ_{pigeon}^*, and the pink zone is the estimated victory zone VZ_{pigeon}. The simulation results demonstrate that there is no initial position guaranteed to win outside the estimated victory zone for the pigeon, and the victory can not always be guaranteed within the estimated victory zone, i.e., $VZ_{\text{pigeon}}^* \leq VZ_{\text{pigeon}}$. A large number of simulation results verify the correctness of the conclusion, meanwhile, it can be seen that the real victory zone is random and uncertain, and the analytical solution can not be given.

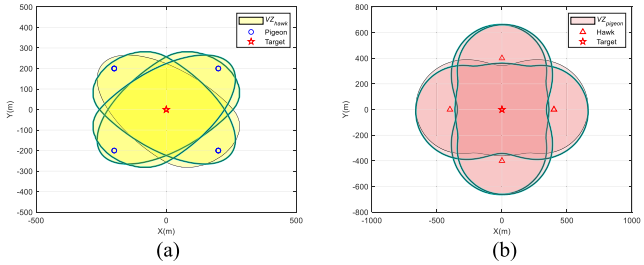

Fig. 7. Estimated victory zone under multiple players. (a) Hawk's estimated victory zone in the presence of four pigeons. (b) Pigeon's estimated victory zone in the presence of four hawks.

Further, the theorem for the hawk-pigeon game can be given as follows:

Theorem 2: Consider the hawk-pigeon game (7)–(21) with N_H hawks and N_P pigeons. $I_H = \{1, \ldots, N_H\}$, $I_P = \{1, \ldots, N_p\}$. The number of target pigeons selected by the hawks is $N_{TP}, N_{TP} \leq N_P$. Given the initial positions of N_P pigeons, the initial position of the ith hawk satisfies $\mathbf{p}^{i0}_{\text{hawk}} \in \bigcap_{j \in I_P} VZ^j_{\text{hawk}}(i)\ \forall i \in I_H$, where $VZ^j_{\text{hawk}}(i)$ is the ith hawk's estimated victory zone relative to the jth pigeon, then at least N_{TP} pigeons are guaranteed to be captured. Given the initial positions of N_H hawks, if the initial position of the jth pigeon satisfies $\mathbf{p}^{j0}_{\text{pigeon}} \notin \bigcup_{i \in I_H} VZ^i_{\text{pigeon}}(j)\ \forall j \in I_P$, where $VZ^i_{\text{pigeon}}(j)$ is the jth pigeon's estimated victory zone relative to the ith hawk, then at least N_{TP} pigeons are guaranteed to be captured.

Proof: Let I_{TP} be the target pigeon set selected by the hawks, then the number of pigeons in I_{TP} is N_{TP}. According to the conclusion that the real victory zone of the hawk is at least the estimated victory zone, and the real victory zone of the pigeon is, at best, the estimated victory zone, it can be obtained that

$$\begin{aligned}
&\mathbf{p}^{i0}_{\text{hawk}} \in \bigcap_{j \in I_P} VZ^j_{\text{hawk}}(i)\ \forall i \in I_H \\
&\Rightarrow \forall j \in I_P, \mathbf{p}^{i0}_{\text{hawk}} \in VZ^j_{\text{hawk}}(i)\ \forall i \in I_H \\
&\Rightarrow \exists j \in I_P, \mathbf{p}^{i0}_{\text{hawk}} \in VZ^j_{\text{hawk}}(i)\ \forall i \in I_H \\
&\Rightarrow \forall j \in I_{TP}, \mathbf{p}^{i0}_{\text{hawk}} \in VZ^j_{\text{hawk}}(i)\ \forall i \in I_H. \qquad (35)
\end{aligned}$$

It can be proved that if $\mathbf{p}^{i0}_{\text{hawk}} \in \bigcap_{j \in I_P} VZ^j_{\text{hawk}}(i)\ \forall i \in I_H$, at least N_{TP} pigeons are guaranteed to be captured

$$\begin{aligned}
&\mathbf{p}^{j0}_{\text{pigeon}} \notin \bigcup_{i \in I_H} VZ^i_{pigeon}(j)\ \forall j \in I_P \\
&\Rightarrow \forall i \in I_H, \mathbf{p}^{j0}_{\text{pigeon}} \notin VZ^i_{\text{pigeon}}(j)\ \forall j \in I_P \\
&\Rightarrow \exists i \in I_H, \mathbf{p}^{j0}_{\text{pigeon}} \notin VZ^i_{\text{pigeon}}(j)\ \forall j \in I_P \\
&\Rightarrow \exists i \in I_H, \mathbf{p}^{j0}_{\text{pigeon}} \notin VZ^i_{\text{pigeon}}(j)\ \forall j \in I_{TP}. \qquad (36)
\end{aligned}$$

It can be proved that if $\mathbf{p}^{j0}_{\text{pigeon}} \notin \bigcup_{i \in I_H} VZ^i_{\text{pigeon}}(j), \forall j \in I_P$, at least N_{TP} pigeons are guaranteed to be captured.

To make it more intuitive, the following examples are given. Fig. 7(a) gives the hawk's estimated victory zone in the presence of four pigeons, and the overlap of four yellow zones is corresponding to $\bigcap_{j \in I_p} VZ^j_{\text{hawk}}$. The hawk initially located in $\bigcap_{j \in I_p} VZ^j_{\text{hawk}}$ is guaranteed to capture the target pigeon. Fig. 7(b) gives the pigeon's estimated victory zone in the presence of four hawks, and the full coverage of four pink zones is corresponding to $\bigcup_{i \in I_h} VZ^i_{\text{pigeon}}$. The target pigeon whose initial position is outside $\bigcup_{i \in I_h} VZ^i_{\text{pigeon}}$ is guaranteed to be captured. ■

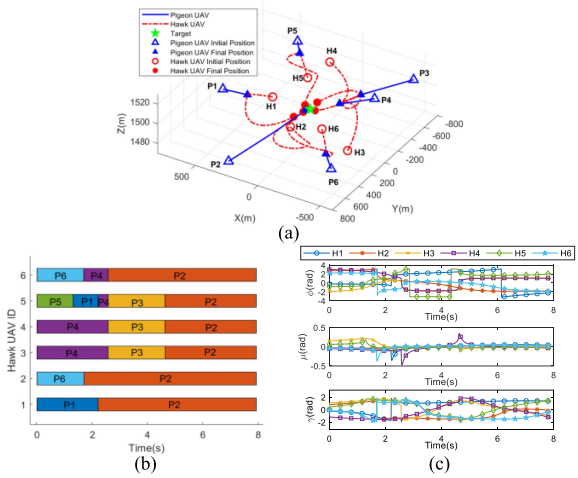

Fig. 8. Results of the hawk-pigeon game (case 1: 6-versus-6). (a) 3-D trajectories, hawk UAVs won and captured six pigeon UAVs with 7.91 s. (b) Hawk UAVs target selection. (c) Angles of hawk UAVs.

V. Comparative Simulation Analysis

To validate the efficacy and superiority of the proposed approach, comparative simulations have been carried out. A UAV swarm target defense scenario in the unbounded space is considered, where there are two groups of adversarial UAV swarms and a fixed target asset. The hawk UAVs are regarded as defenders and aim to intercept all pigeon UAVs to prevent them from approaching the target. The pigeon UAVs are regarded as attackers, and their purpose is to capture the target as quickly as possible while avoiding the hawk UAVs threat. Both UAVs are given the same performance, and there is no difference in the sensing and attack abilities of the UAVs, except that the maximum speed of the hawk UAV is larger than that of the pigeon UAV.

In comparative experiments, the approach in [23] named H-L is applied to the defender UAV swarm to highlight the superiority of the attacker strategies in this article. Besides, the attack strategy in [7] is applied to the attacker UAV swarm to highlight the superiority of the defender strategies in this article.

The simulation parameters are given in Table I. The position of the target is $\mathbf{p}_T = [0, 0, 1500]\text{m}$, the initial positions of hawk and pigeon UAVs are generated randomly in the task area. The simulation time is 10 s, and the time step is 0.01 s.

A. Case1: Engagement Around the Target

When the number of hawk UAVs is equal to that of pigeon UAVs, the results are shown in Figs. 8 and 9. For the hawk-pigeon game, the hawk UAVs selected and switched the target efficiently and finally captured all pigeon UAVs with 7.91s. For H–L, six

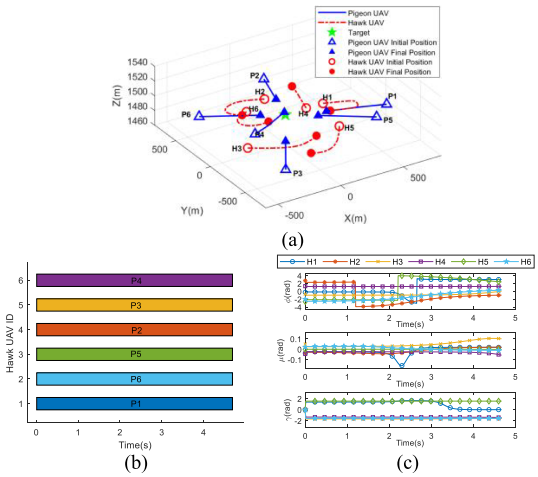

Fig. 9. Results of H-L (Case 1: 6-versus-6). (a) 3-D trajectories, pigeon UAVs won without losses in 4.67 s. (b) Hawk UAVs target selection. (c) Angles of hawk UAVs.

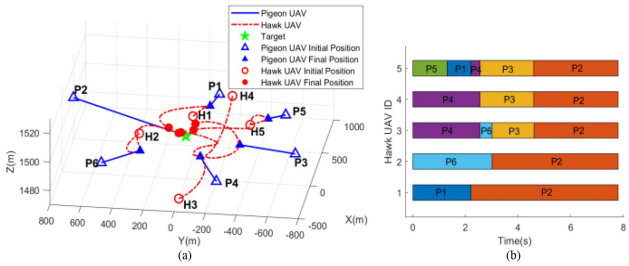

Fig. 10. Results of the hawk-pigeon game (case 1: 5-versus-6). (a) 3-D trajectories, hawk UAVs won and captured six pigeon UAVs with 7.79s. (b) Hawk UAVs target selection.

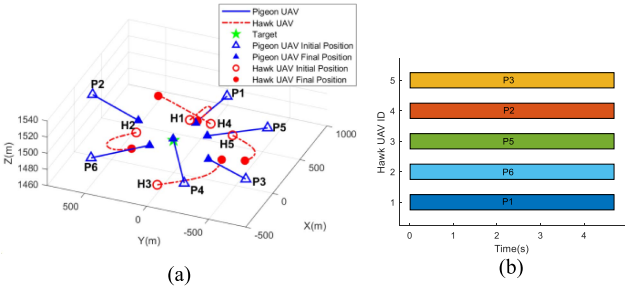

Fig. 11. Results of H–L (case 1: 5-versus-6). (a) 3-D trajectories, pigeon UAVs won without losses in 4.67s. (b) Hawk UAVs target selection.

hawk UAVs targeted six different pigeon UAVs, but none of the hawk UAVs pursuits successfully the target pigeon UAV. Compared with the proposed hawk-inspired attack tactics and control strategy, the H–L approach performs not very well.

When the number of hawk UAVs is fewer than pigeon UAVs, the results are shown in Figs. 10 and 11. For the hawk-pigeon game, despite the quantity inferior, the hawk UAV swarm still captured successfully all pigeon UAVs with 7.79 s, which attributes to the hawk's attack tactics and precise pursuit strategy. However, the hawk UAVs utilizing the H–L approach failed to

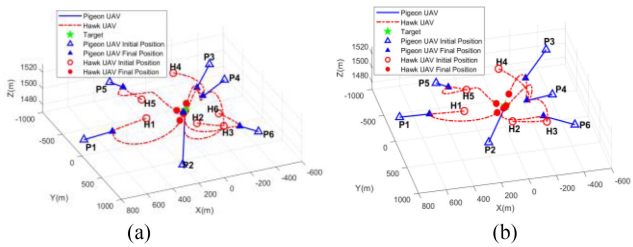

Fig. 12. Defenders of this article versus attackers of [7]. (a) 6-versus-6. (b) 5-versus-6.

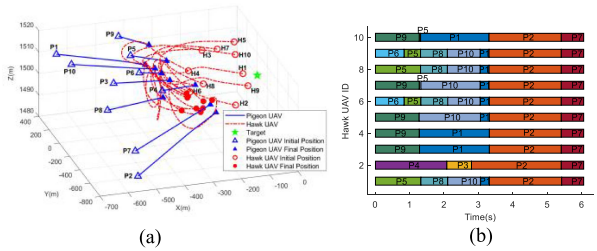

Fig. 13. Results of the hawk-pigeon game (case 2: 10-versus-10). (a) 3-D trajectories, hawk UAVs won and captured ten pigeon UAVs with 6.04s. (b) Hawk UAVs target selection.

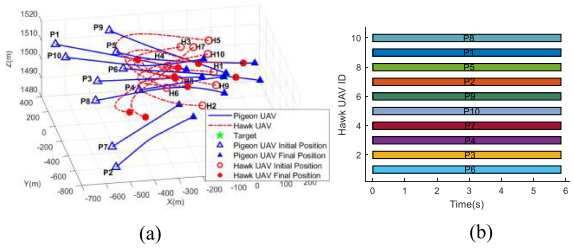

Fig. 14. Results of H-L (case 2: 10- versus-10). (a) 3-D trajectories, pigeon UAVs won without losses in 5.83 s. (b) Hawk UAVs target selection.

intercept any pigeon UAV. The pigeon UAVs adopt the attack strategy of [7], the results are shown in Fig. 12. In the scenarios of 6- versus-6 and 5- versus-6, the hawk UAVs won with 7.87 s and 7.75 s, respectively.

B. Case 2: Engagement on One Side of the Target

In case 2, the results are shown in Figs. 13–17. It can be seen that the efficiency of the proposed approach is not affected by the increasing number of players. For the hawk-pigeon game, despite the numerical and initial position disadvantages, the hawk UAV swarm can still intercept all pigeon UAVs, which is enough to see the effectiveness of the hawk-inspired defender strategy, i.e., the target selection tactics and control strategy. Similarly, the hawk UAVs using the H-L approach hardly work well due to the inappropriate target-matching algorithm and the inflexible pursuit control strategy facing the pigeon UAVs. The pigeon UAVs adopt the attack strategy of [7], the results are shown in Fig. 17. In the scenarios of 10-versus-10 and 8-versus-10, the hawk UAVs won with 6.03s and 8.75s, respectively.

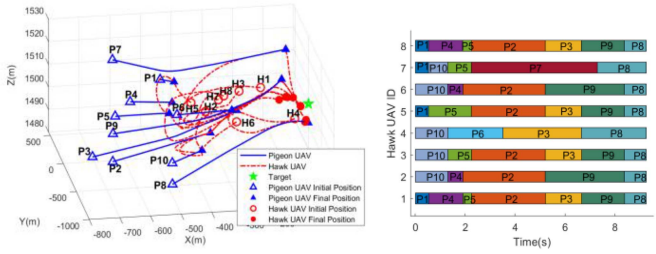

(a) (b)

Fig. 15. Results of the hawk-pigeon game (case 2: 8-versus-10). (a) 3-D trajectories, hawk UAVs won and captured ten pigeon UAVs with 9.24 s. (b) Hawk UAVs target selection.

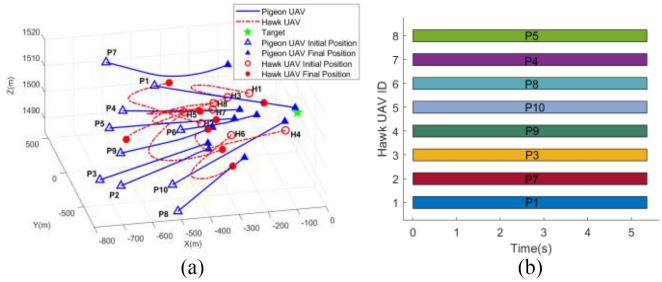

(a) (b)

Fig. 16. Results of H–L (case 2: 8- versus-10). (a) 3-D trajectories, pigeon UAVs won without losses in 5.34 s. (b) Hawk UAVs target selection.

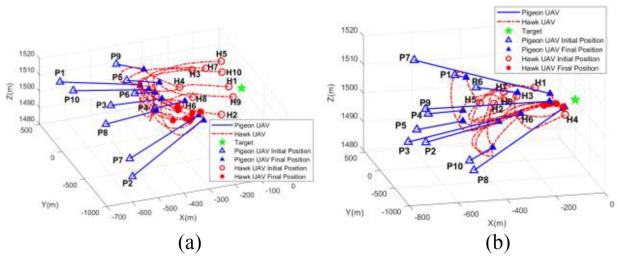

(a) (b)

Fig. 17. Defenders of this article versus attackers of [7]. (a) 10- versus-10. (b) 8- versus-10.

VI. Conclusion

A UAV swarm target defense approach based on the hawk-pigeon game was proposed in this article. The hawk-pigeon game was formulated as a multiplayer TAD game. The strategies of the defender UAVs and attacker UAVs were designed based on hawk and pigeon intelligence behaviors, respectively. It was noted that the proposed hawk-pigeon game approach, requiring almost no parameter tuning with stable good performance, was not affected by the number of UAVs, and was extended to larger-scale UAV swarm combat missions with low computational complexity. Especially, the attack tactics and pursuit control strategy of the defender UAVs show significant advantages, even when faced with outnumbered opponents. The targeting mechanism of the defender UAVs performs better with the increasing number of opponents. Moreover, substantial simulation results indicate that the outcome of engagement and the activity time were mainly affected by the initial positions of two sides and have little to do with the number of UAVs (under the condition that the number of two sides differs not greatly).

Our future work will focus on the attacker's antiattack ability, the defender's avoiding tendency, and the attack-defense strategies conversion.

References

[1] L. G. Strickland, C. E. Pippin, and M. C. Gombolay, "Learning to steer swarm-vs.-swarm engagement," in *Proc. AIAA Scitech Forum*, 2021, Art. no. 0165.

[2] W. Wang, C. Fang, and T. Liu, "Multiperiod unmanned aerial vehicles path planning with dynamic emergency priorities for geohazards monitoring," *IEEE Trans. Ind. Inform.*, vol. 18, no. 12, pp. 8851–8859, Dec. 2022.

[3] L. Sun, L. Wan, and X. Wang, "Learning-based resource allocation strategy for industrial IoT in UAV-enabled MEC systems," *IEEE Trans. Ind. Inform.*, vol. 17, no. 7, pp. 5031–5040, Jul. 2021.

[4] W. J. Yun et al., "Cooperative multiagent deep reinforcement learning for reliable surveillance via autonomous multi-UAV control," *IEEE Trans. Ind. Inform.*, vol. 18, no. 10, pp. 7086–7096, Oct. 2022.

[5] E. Garcia, D. Tran, D. Casbeer, D. Milutinovic, and M. Pachter, "Beyond visual range tactics," in *Proc. AIAA Scitech Forum*, 2021, Art. no. 1229.

[6] J. R. Bertram and P. Wei, "An efficient algorithm for multiple-pursuer-multiple-evader pursuit/evasion game," in *Proc. AIAA Scitech Forum*, 2021, Art. no. 1862.

[7] E. Garcia, D. W. Casbeer, and M. Pachter, "Active target defense using first order missile models," *Automatica*, vol. 78, pp. 139–143, Jan. 2017.

[8] E. Garcia, D. W. Casbeer, and M. Pachter, "Cooperative target protection from a superior attacker," *Automatica*, vol. 131, May 2021, Art. no. 109696.

[9] E. Garcia, D. W. Casbeer, and M. Pachter, "Design and analysis of state-feedback optimal strategies for the differential game of active defense," *IEEE Trans. Autom. Control*, vol. 64, no. 2, pp. 553–568, Feb. 2019.

[10] L. Liang, F. Deng, M. Lu, and J. Chen, "Analysis of role switch for cooperative target defense differential game," *IEEE Trans. Autom. Control*, vol. 66, no. 2, pp. 902–909, Feb. 2021.

[11] L. Liang, F. Deng, Z. H. Peng, X. X. Li, and W. Z. Zha, "A differential game for cooperative target defense," *Automatica*, vol. 102, pp. 58–71, Jan. 2019.

[12] W. Zha, J. Chen, Z. Peng, and D. Gu, "Construction of barrier in a fishing game with point capture," *IEEE Trans. Cybern.*, vol. 47, no. 6, pp. 1409–1422, Jun. 2017.

[13] X. Fang, C. Wang, L. Xie, and J. Chen, "Cooperative pursuit with multi-pursuer and one faster free-moving evader," *IEEE Trans. Cybern.*, vol. 52, no. 3, pp. 1405–1414, Mar. 2022.

[14] J. L. Salmon, L. C. Willey, D. Casbeer, E. Garcia, and A. V. Moll, "Single pursuer and two cooperative evaders in the border defense differential game," *J. Aerosp. Inform. Syst.*, vol. 17, no. 5, pp. 229–238, May 2020.

[15] W. L. Scott and N. E. Leonard, "Optimal evasive strategies for multiple interacting agents with motion constraints," *Automatica*, vol. 94, pp. 26–34, Apr. 2018.

[16] E. Garcia, D. W. Casbeer, A. V. Moll, and M. Pachter, "Multiple pursuer multiple evader differential games," *IEEE Trans. Autom. Control*, vol. 66, no. 5, pp. 2345–2350, May 2021.

[17] M. Chen, Z. Zhou, and C. J. Tomlin, "Multiplayer reach-avoid games via pairwise outcomes," *IEEE Trans. Autom. Control*, vol. 62, no. 3, pp. 1451–1457, Mar. 2017.

[18] R. Yan, X. M. Duan, Z. Y. Shi, Y. S. Zhong, and F. Bullo, "Matching-based capture strategies for 3D heterogeneous multiplayer reach-avoid differential games," *Automatica*, vol. 140, Mar. 2022, Art. no. 110207.

[19] J. T. English, "A defender-aware attacking guidance policy for the TAD differential game," M.S. thesis, Russ College Eng. Tech., Ohio Univ., Columbus, OH, USA, 2020.

[20] B. Vlahov, E. Squires, L. Strickland, and C. Pippin, "On developing a UAV pursuit-evasion policy using reinforcement learning," in *Proc. IEEE 17th Int. Conf. Mach. Learn. Appl.*, 2018, pp. 859–864.

[21] L. Strickland, M. Day, K. DeMarco, E. Squires, and C. Pippin, "Responding to unmanned aerial swarm saturation attacks with autonomous counter-swarms," *Proc. SPIE*, vol. 10635, 2018. Art. no. 106350Y.

[22] D. M. Stipanović, A. Melikyan, and N. Hovakimyan, "Guaranteed strategies for nonlinear multi-player pursuit-evasion games," *Int. Game Theory Rev.*, vol. 12, no. 1, pp. 1–17, 2021.

[23] V. S. Chipade and D. Panagou, "Multiplayer target-attacker-defender differential games: Pairing allocations and control strategies for guaranteed intercept," in *Proc. AIAA Scitech Forum*, 2019, Art. no. 0658.
[24] S. Zhang, M. Y. Liu, X. K. Lei, P. P. Yang, Y. K. Huang, and R. Clark, "Group chase and escape with prey's anti-attack behavior," *Phys. Lett. A*, vol. 383, Aug. 2019, Art. no. 125871.
[25] N. Paul and D. Ghose, "Longitudinal acceleration-based guidance law inspired from hawk's attack against a maneuvering target," in *Proc. AIAA Scitech Forum*, 2022, Art. no. 0540.
[26] M. Z. Huo, H. B. Duan, and Y. M. Fan, "Pigeon-inspired circular formation control for multi-UAV system with limited target information," *Guid. Navig. Control*, vol. 1, no. 1, Mar. 2021, Art. no. 2150004.
[27] C. H. Brighton, A. L. R. Thomas, and G. K. Taylor, "Terminal attack trajectories of peregrine falcons are described by the proportional navigation guidance law of missiles," *Proc. Nat. Acad. Sci.*, vol. 114, no. 51, pp. 13495–13500, Aug. 2017.
[28] C. H. Brighton, K. E. Chapman, N. C. Fox, and G. K. Taylor, "Attack behaviour in naive gyrfalcons is modelled by the same guidance law as in peregrine falcons, but at a lower guidance gain," *J. Exp. Biol.*, vol. 224, Jan. 2021, Art. no. jeb238493.
[29] D. W. E. Sankey, R. F. Storms, R. J. Musters, T. W. Russell, C. K. Hemelrijk, and S. J. Portugal, "Absence of 'selfish herd' dynamics in bird flocks under threat," *Curent Biol.*, vol. 31, pp. 3192–3198, Jul. 2021.
[30] H. X. Qiu and H. B. Duan, "Pigeon interaction mode switch-based UAV distributed flocking control under obstacle environments," *ISA Trans.*, vol. 71, pp. 93–102, Jul. 2017.
[31] F. Austin, G. Carbone, M. Falco, H. Hinz, and M. Lewis, "Game theory for automated maneuvering during air-to-air combat," *J. Guid. Control Dyn.*, vol. 13, no. 6, pp. 1143–1149, Nov. 1990.
[32] J. Demšar, C. K. Hemelrijk, H. Hildenbrandt, and I. L. Bajec, "Simulating predator attacks on schools: Evolving composite tactics," *Ecol. Model.*, vol. 304, pp. 22–33, Mar. 2015.
[33] W. Ruan, H. Duan, and Y. Deng, "Autonomous maneuver decisions via transfer learning pigeon-inspired optimization for UCAVs in dogfight engagements," *IEEE/CAA J. Automatica Sinica*, vol. 9, no. 9, pp. 1639–1657, Sep. 2022.
[34] C. H. Brighton and G. K. Taylor, "Hawks steer attacks using a guidance system tuned for close pursuit of erratically manoeuvring targets," *Nature Commun.*, vol. 10, Jun. 2019, Art. no. 2462.
[35] G. Vásárhelyi, C. Virágh, G. Somorjai, T. Nepusz, A. E. Eiben, and T. Vicsek, "Optimized flocking of autonomous drones in confined environments," *Sci. Robot.*, vol. 3, no. 20, Jul. 2018, Art. no. eaat3536.
[36] N. A. Shneydor, "Pure pursuit," in *Missile Guidance and Pursuit: Kinematics, Dynamics and Control*, 1st ed. Cambridge, U.K.: Woodhead Publ., 1998, pp. 47–76.

Wanying Ruan received the B.S. and M.S. degrees in electrical engineering and automation from Shijiazhuang Tiedao University, Shijiazhuang, China, in 2015 and 2019, respectively. She is currently working toward the Ph.D. degree in navigation, guidance and control with the Bio-Inspired Autonomous Flight Systems Research Group, State Key Laboratory of Virtual Reality Technology and Systems, School of Automation Science and Electrical Engineering, Beihang University, Beijing, China.

Her research interests include bio-inspired intelligence, unmanned aerial vehicle swarm autonomous control and decision, and unmanned aerial vehicle group game.

Yongbin Sun (Member, IEEE) received the B.S. degree in automation from Shandong University, Jinan, China, in 2015, and the Ph.D. degree in navigation, guidance and control from Beihang University, Beijing, China, in 2021.

He is currently an Assistant Professor with the Bio-Inspired Autonomous Flight Systems Research Group, School of Automation Science and Electrical Engineering, Beihang University, Beijing, China.

His current research interests include multi-UAVs cooperative control and bionic vision-based navigation.

Yimin Deng received the B.S. and Ph.D. degrees in control science and engineering from the School of Automation Science and Electrical Engineering, Beihang University, Beijing, China, in 2011 and 2017, respectively.

He is currently an Associate Professor with the Bio-Inspired Autonomous Flight Systems Research Group, School of Automation Science and Electrical Engineering, Beihang University. He was enrolled in the Young Elite Scientists Sponsorship Program by Chinese Association for Science and Technology, and Young Top Talent Support Program by Beihang University. His research interests include biological computer vision and autonomous flight control.

Haibin Duan (Senior Member, IEEE) received the Ph.D. degree in control theory and control engineering from Nanjing University of Aeronautics and Astronautics, Nanjing, China, in 2005.

He is currently a Full Professor with the School of Automation Science and Electrical Engineering, Beihang University, Beijing, China. He is the Vice Director of the State Key Laboratory of Virtual Reality Technology and Systems, and the Head of the Bio-Inspired Autonomous Flight Systems Research Group, Beihang University, Beijing, China. He has authored or coauthored more than 100 publications in journals. His current research interests are bio-inspired intelligence, biological computer vision and unmanned systems swarm autonomous control.

Dr. Duan was the recipient of the National Science Fund for Distinguished Young Scholars of China in 2014. He is also enrolled in the Chang Jiang Scholars Program of China in 2018, Scientific and Technological Innovation Leading Talent of "Ten Thousand Plan"-National High Level Talents Special Support Plan in 2017, and Top-Notch Young Talents Program of China in 2012, Program for New Century Excellent Talents in University of China in 2010, and Beijing NOVA Program in 2007. He is the Editor-in-Chief for *Guidance, Navigation and Control*, an Associate Editor for IEEE TRANSACTIONS ON CYBERNETICS, and IEEE TRANSACTIONS ON CIRCUITS AND SYSTEMS II: EXPRESS BRIEFS.